Carbohydrate Polymers 102 (2014) 884–892

Contents lists available at ScienceDirect

Carbohydrate Polymers

journal homepage: www.elsevier.com/locate/carbpol

Electrospun antibacterial polyurethane–cellulose acetate–zein composite mats for wound dressing

Afeesh Rajan Unnithan[a,*], Gopalsamy Gnanasekaran[b], Yesupatham Sathishkumar[c], Yang Soo Lee[c], Cheol Sang Kim[a,*]

[a] Bionano Systems Engineering Department, Chonbuk National University, Jeonju 561-756, Republic of Korea
[b] Department of Molecular Medicine Clinical Vaccine R&D Center, Chonnam National University, Hwasun, South Korea
[c] College of Agriculture and Life Sciences, Chonbuk National University, Jeonju 561-756, Republic of Korea

ARTICLE INFO

Article history:
Received 4 September 2013
Received in revised form 16 October 2013
Accepted 21 October 2013
Available online 26 October 2013

Keywords:
Wound dressing
Electrospinning
Antibacterial
Nanofiber
Tissue engineering
Zein

ABSTRACT

In this study, an antibacterial electrospun nanofibrous scaffolds with diameters around 400–700 nm were prepared by physically blending polyurethane (PU) with two biopolymers such as cellulose acetate (CA) and zein. Here, PU was used as the foundation polymer, was blended with CA and zein to achieve desirable properties such as better hydrophilicity, excellent cell attachment, proliferation and blood clotting ability. To prevent common clinical infections, an antimicrobial agent, streptomycin sulfate was incorporated into the electrospun fibers and its antimicrobial ability against the gram negative and gram positive bacteria were examined. The interaction between fibroblasts and the PU–CA and PU–CA–zein-drug scaffolds such as viability, proliferation, and attachment were characterized. PU–CA–zein-drug composite nanoscaffold showed enhanced blood clotting ability in comparison with pristine PU nanofibers. The presence of CA and zein in the nanofiber membrane improved its hydrophilicity, bioactivity and created a moist environment for the wound, which can accelerate wound recovery.

1. Introduction

Preventing the wound infection is the major difficulty in the field of wound care management, because such infections can cause exudate formation, delay the wound healing and it can result in disfiguring or even can threaten life (Jayakumar, Prabaharan, Sudheesh, Nair, &Tamura, 2011). Any open skin lesion is a potential invasion site for microorganisms and the adequate wound management is necessary to prevent infection (Madhumathi et al., 2010). Microbes are the major reason for infection and the presence of the same is high in and around us. Once entered into the body, these microbes grow immediately and start to form colonies. Through the open wounds these microbes can easily access into the body and can reach into deeper portions of the tissue and, can lead in to internal infections (Sudheesh et al., 2012). The remedy for the above-mentioned harms would be the use of wound dressing materials that can achieve rapid healing while minimizing infection. Ideal antimicrobial dressings should have a number of features such as provision of a moist environment to enhance healing, and broad-spectrum antimicrobial activity, including activity against antibiotic-resistant bacteria. Therefore, immediate care of skin wounds is important for prevention of microbial infection and trans-epidermal water loss leading to acceleration of wound regeneration (Jayakumar, Menon, Manzoor, Nair, & Tamura, 2010).Electrospinning is a simple, versatile, cost-effective, and scalable system using high voltage electrical field to generate aligned or random nanofibers from several synthetic and natural polymers (Lakshmi, Shalumon, Sreeja, Jayakumar, & Nair, 2010). The bioactive antibacterial dressing materials made from e-spun nanofibers are influenced by many factors, such as polymer types and their properties (i.e., hydrophilicity and hydrophobicity), drug solubility and drug–polymer adhesion and mat structures. The high surface area and the short diffusion passage length can give the nanofiber drug system a higher overall release rate than the bulk materials (Fang, Niu, Lin, & Wang, 2008). Most importantly encapsulated drug within the nanofiber matrix can also give a good control for either a sustained release or a burst release to the wound surface.

PU is a commonly used candidate for wound dressing applications. PU is frequently used in wound dressings because of its good barrier properties and oxygen permeability. Research has reported that semi-permeable dressings, many of which are PU, enhance wound healing (Afeesh et al., 2012). PU is a soft and hydrophobic polymer. If it is used alone for a dressing material, these two properties would be drawbacks because the dressing may be too

* Corresponding authors. Tel.: +82 63 270 4284; fax: +82 63 270 2460.
E-mail addresses: afeesh@jbnu.ac.kr, afeeshnano@gmail.com (A.R. Unnithan), chskim@jbnu.ac.kr (C.S. Kim).

0144-8617/$ – see front matter © 2013 Elsevier Ltd. All rights reserved.
http://dx.doi.org/10.1016/j.carbpol.2013.10.070

soft for clinical handling and its hydrophobic property may prevent fluid exuding from wound surface. Cellulose acetate (CA) is a commonly used biopolymer. CA is highly hydrophilic, with good liquid transport and water absorption abilities. Cellulose acetate (CA), the acetate ester of cellulose, has been widely investigated for a wide variety of potential applications in the form of electrospun nanofiber mats because of its advantageous properties, such as good biocompatibility, biodegradability, regenerative properties, high affinity with other substances, high modulus, and adequate flexural and tensile strength (Glasser, 2004). However, because of its low breaking stress, strain, and poor resistance, CA is not suitable for clinic use if it is used alone as biomedical material.

Zein is one of the main plant proteins and has been used to develop biodegradable films and other substrates for tissue engineering and other medical applications (Jiang, Reddy, & Yang, 2010). Studies (Kanjanapongkul, Wongsasulak, & Yoovidhya, 2010) have shown that it is easy to be electrospun into fibers. Zein exhibits various interesting properties such as toughness, flexibility, compressibility, glossiness, resistance to microbial attack (Shukla & Cheryan, 2001) and antioxidant activity (Kong & Xiong, 2006). Zein has also been used as a carrier for drug delivery (Liu, Sun, Wang, Zhang, & Wang, 2005), in food packaging and in scaffolding materials for cell/tissue culture (Gong, Wang, Sun, Xue, & Wang, 2006). All these applications suggest that zein can have wider applications in the biomedical field. Moreover, zein has better biocompatibility and good degradability when compared to those synthetic polymers co-electrospun with PU. Therefore, the co-electrospinning of PU–CA with zein may improve the electrospinnability and result in bio-compatible nanofibrous membranes with enhanced properties.

In this study, PU was used as the foundation polymer, was blended with CA and zein to achieve desirable properties such as better cell viability, cell attachment and proliferation, enhanced blood clotting ability and improved hydrophilicity. The antimicrobial agent streptomycin was incorporated into the electrospun nanofibers, and its antimicrobial ability against the gram negative and gram positive bacteria were examined. The study demonstrates the process, stability, and the characterization of the composite nanofibrous scaffolds. An electrospun nanofiber membrane containing antibiotic agents can be used as a barrier to prevent the post-wound infections. The combination of both of these properties can result in a perfect wound dressing material.

2. Experimental procedure

2.1. Materials and methods

Polyurethane, 10 wt% (PU, Estane® Skythane® X595A-11, Lubrizol) and cellulose acetate, 15 wt% (CA, Sigma Aldrich, Korea, Mw ~30,000) were prepared by dissolving overnight in solvent mixture of *N*,*N* dimethylformamide (DMF, Samchun, Korea) and methyl ethyl ketone/2-butanone (MEK, extra pure, Samchun, Korea) (50/50, wt:wt%). The two polymer solutions were mixed in 1:1, 2:1 and 3:1 ratio for the current study. 2 wt% Zein powder (Sigma Aldrich, USA) has been added to those respective solutions along with 1 wt% streptomycin sulfate (Sigma Aldrich, Germany). The obtained solutions were placed in a plastic syringe tube and fed through a metal capillary (nozzle) with a diameter di = 0.21 mm (21G) attached to a 1-D robot-system that moves laterally and is controlled by the LabVIEW 9.0 software program (National Instrument). The feeding rate was maintained at 0.5 ml/h via a controllable syringe pump. Electrospinning was carried out at a voltage of 18 kV and working distance of 15 cm at room temperature. Finally, the composite nanofiber mats were vacuum dried in an oven at 30 °C for 24 h to remove the residual solvent and this sample was used for further characterizations.

2.2. Characterizations

The morphology of the electrospun composite mats was observed by using scanning electron microscopy (SEM, S-7400, Hitachi, Japan) and field-emission scanning electron microscopy (FE-SEM, Hitachi S-7400, Hitachi, Japan). The bonding configurations of the samples were characterized by means of Fourier-transform infrared (FT-IR) spectroscopy. Mechanical properties were measured with a universal testing machine (AG-5000G, Shimadzu, Japan), under a crosshead speed of 10 mm/min. The samples were prepared in the form of standard dumbbell shaped according to ASTM Standard 638 via die cutting from the mat and tested in machine direction. Wettability was measured by using the deionized water contact angle measurement using contact angle meter (Digidrop, GBX, France). Deionized water was automatically dropped (drop diameter 6 μm) onto the mat.

2.3. Platelet activation study and whole blood clotting assay

The blood clotting studies were done based on reported literature (Ong, Wu, Moochhala, Tan, & Lu, 2008). Blood was drawn from voluntary human ulnar vein using BD Discardit II sterile syringe and mixed with anticoagulant agent acid citrate dextrose at a ratio of 9:1. Triplicate samples were used for this study and pristine PU mat was used as negative control. Later blood was added to each composite nanofiber mats and placed in a 25-mL plastic Petri dish, which was followed by the addition of 10 μL of 0.2 M $CaCl_2$ solutions to initiate blood clotting. These mats were then incubated at 37 °C for 10 min. 15 mL of distilled water was then added drop wise without disturbing the clot. Subsequently, 10 mL of solution was taken from the dishes and was centrifuged at 1000 rpm for 1 min. The supernatant was collected for each sample and kept at 37 °C for 1 h. Two hundred microliters (200 μL) of this solution was transferred to a 96-well plate. The optical density was measured at 530 nm using a plate reader (Dynex Technologies, USA). Platelet rich plasma (PRP) was isolated from the blood by centrifugation of blood at 2500 rpm for 5 min. One hundred microliters (100 μL) of PRP was poured onto the composite nanofiber mats and incubated at 37 °C for 20 min. The composite nanofiber mats were then washed three times with PBS solution and fixed using 0.1% glutaraldehyde solution. The mats were dried and SEM images were taken.

2.4. Cell attachment study

3T3-L1 fibroblasts (preadipocytes, Korean Cell Line Bank, Korea) were initially maintained in Dulbecco's modified Eagle's medium supplemented with 10% fetal bovine serum, 2 mM glutamine, 100 μg/mL penicillin, and 100 μg/mL streptomycin in a humidified atmosphere of 95% air/5% CO_2 at 37 °C. The electrospun scaffolds on cover slips were ultraviolet (UV) sterilized for 90 min, rinsed in phosphate-buffered saline (PBS) and soaked in cell culture medium overnight prior to cell seeding to facilitate protein adsorption and cell attachment. The fibroblasts were separated by trypsinization, centrifuged, counted using a haemocytometer and seeded on the scaffolds at a cell density of 2×10^4 cells/well and incubated at conditions suitable for cell growth. In order to observe cell attachment manner on composite nanofibers, chemical fixation of cells was carried out in each sample. After 1, 3 and 5 days of incubation, the scaffolds were rinsed twice with PBS and subsequently fixed in 2.5% glutaraldehyde for 1 h. After that the samples were rinsed with distilled water and then dehydrated with graded concentration of ethanol, i.e., 20, 30, 50, 70 and 100% ethanol for 10 min each. Finally, the samples were kept in a vacuum oven and then sputter coated with gold for the cell morphology observation by using SEM.

2.5. MTT test

The viability of cultured fibroblasts was monitored on the third, sixth and ninth day of culture using the colorimetric MTT assay (Sigma, USA). The scaffolds were washed twice with PBS and were then treated with approximately 50 μl of the MTT solution (DMEM); the scaffolds, after mixing of the contents by side-tapping, were incubated at 37 °C for 2 h. The scaffolds containing MTT–cell mixtures were gently rocked to deposit the cells. The supernatant MTT solution was pipette out and then acid–isopropanol (95 mL isopropanol with 5 ml 3 N HCl) was added to the colored cell deposit. After gently mixing the acid–alcohol-treated scaffolds was then allowed to react for 5 min. One hundred microliter of the purple–blue colored supernatant that contained the solubilized formazan in each sample was added to a well in a 96-well plate for spectrophotometric analysis at 580 nm in an ELISA reader. The cell viability was obtained by comparing the absorbance of cells cultured on the nanofibers scaffold to that of control well containing cells. The results were expressed as the mean ± standard error of the mean. The data were analyzed via the Student's *t*-test and repeated measures of analyses of variance (ANOVA) test. A probability of less than 0.01 was considered to be statistically significant.

2.6. Antibacterial assessment

2.6.1. Microbial strains and culturing conditions

The following micro-organisms were used for antibacterial assessment study: *Escherichia coli* K12-MG1655, *Salmonella typhimurium*, *Vibrio vulnificus* CMCP6, *Staphylococcus aureus* ATCC 25923 and *Bacillus subtilis*. Preparation of bacterial inoculum as follows: the gram-negative *E. coli*, *S. typhimurium* and *V. vulnificus* and gram-positive bacteria *S. aureus* and *B. subtilis* were precultured in Luria-Bertani Broth (LB) overnight in a rotary shaker at 37 °C, centrifuged at 13,000 rpm for 2 min, pellet was suspended in sterile water and the cell density was standardized spectrophotometrically (A570 nm). The 100 μl of diluted bacterial suspension (10^8 cells/ml) was seeded into respective medium in duplicate by spread plate method. The nutrient agar was used for *S. aureus* and *B. subtilis* and MacConkey agar used for *E. coli*. The thiosulfate citrate bile salts sucrose agar (TCBS) was selective for *Vibrio* and Salmonella Shigella agar (SS) for *Salmonella*.

2.6.2. Antibacterial activity measurement

An inhibitory test of PU–CA–zein nanofibers containing drug, PU–zein and PU were tested by the disk diffusion method (Bauer, Kirby, Sherris, & Turck, 1996). The nanofiberous mats, PU–CA–zein-drug, PU–zein and pristine PU, were cut into small circular discs of diameter around 5 mm each and denoted as A, B and C, respectively. These discs were put on the surface of the Petri dishes. The inhibition zones were estimated after 0-240 min. PU–zein loaded discs and PU only discs were placed as control discs on tested organism seeded plates. The antibacterial activity plates were incubated at 37 °C. The diameters of the inhibition zones were measured in diameter with transparent ruler.

2.6.3. Protocol for fixation of bacteria on nanofibers

Nanofibers were cut into appropriate pieces and placed on Petri plates. Negative control (without drug) was also treated same as the test sample. Overnight bacterial culture was added on to the material and allowed to stand for 4 h for the bacteria to attach and react. Primary fixation was done with 2.5% gluteraldehyde (Daejung, Gyonggi-do, Korea) buffered with 0.01 M phosphate buffered saline (Sigma) for 6 h. Post fixation with 1% aqueous solution of osmium tetroxide (TEDPELLA, Inc., CA, USA) overnight. Samples were dehydrated with 20%, 30%, 40%, 50%, 60%, 70%, 80%, 90%, 100%, 100%, 100% ethanol (Daejung, Gyonggi-do, Korea) 5 min each. Material was kept in dessicator overnight to ensure that material is dry. Samples were placed on stub-carbon electroconductive tape Sputter coated with gold using polaron SC7640 20 mA for 80 s and examined under SEM (Hitachi S-3000N, Japan).

3. Results and discussions

3.1. Morphological analysis and characterizations

The morphology of the nanofiber membranes was shown in Fig. 1. Fig. 1(A) shows the SEM image of pristine PU nanofibers. Fig. 1(B) and (C) shows the SEM images of electrospun PU–CA (1:1) and PU–CA (2:1), respectively. The SEM image of bead free PU–CA (3:1) nanofibers was shown in Fig. 1(D). The formation of beaded fibers in 1:1 and 2:1 ratios may be possibly due to the different surface tension of CA component from PU in blend polymer solution, then causing different stretching time from droplet to fiber during e-spinning. So 3:1 ratio has been finalized for this study and Fig. 1(E) and (F) represents the SEM images of PU–CA (3:1) with

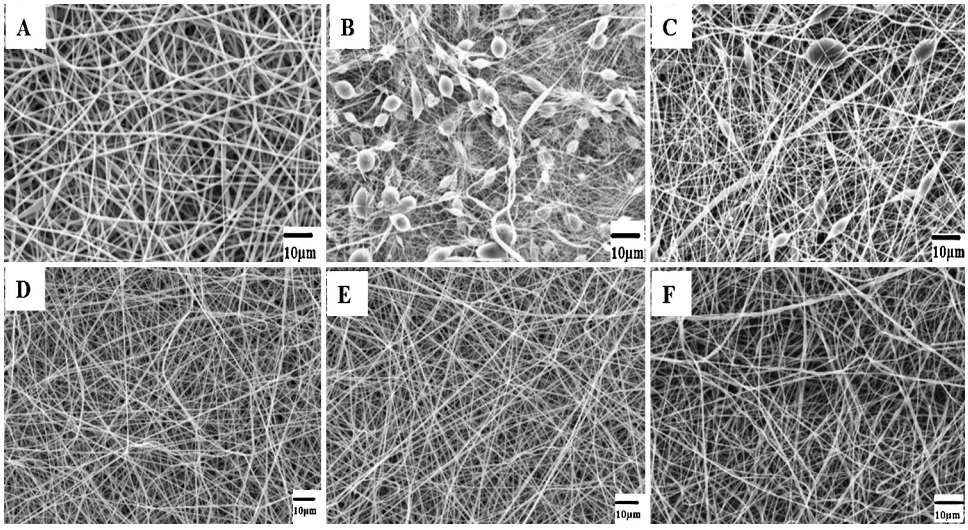

Fig. 1. SEM images of electrospun (A) PU, (B) PU–CA (1:1), (C) PU–CA (2:1), (D) PU–CA (3:1), (E) PU–CA–zein and (F) PU–CA–zein-drug nanofibrous mat.

2 wt% zein (PU–CA–zein) and PU–CA–zein loaded with streptomycin (PU–CA–zein-drug). It can be observed that these randomly oriented as-spun nanofibers exhibited bead-free, smooth surface with almost uniform diameters along their lengths and the diameters of these composite nanofibers were determined to be in the range of 400–700 nm.

FTIR was used to characterize the intermolecular interactions of physical mixture. The spectra of PU, PU–CA–zein and PU–CA–zein-drug loaded nanofibers are shown in Fig. 2. The spectroscopy of electrospun polyurethane has characteristic absorption band at 3320, 2960, 1710, 1530, 1220, 1110 and 777 cm^{-1}, which represents $\upsilon_{(N-H)}$, $\upsilon_{(C-H)}$, $\upsilon_{(C-O)}$, $\upsilon_{(C-C)}$, $\upsilon_{(C-C)}$, $\upsilon_{(C-O)}$, $\upsilon_{(C-H)}$ on substituted benzene, respectively (Jiang, Yuan, Li, & Chow, 2006). The structure of the zein is characterized by typical absorption bands at 1650 cm^{-1} (amide I) and 1536 cm^{-1} (amide II) (Forato et al., 2004). The characteristic adsorption peaks of CA at 1745 cm^{-1} ($\upsilon_{C=O}$) and 1235 cm^{-1} (υ_{C-O-C}) were observed (Yu et al., 2013). The typical absorption band obtained for streptomycin with the peak at a wave number in the vicinity of 1650 cm^{-1} (Richard & Shama, 2005). It can be seen that all the characteristic peaks of PU, CA, zein and drug were visible in PU–CA–zein-drug composite nanofibers and some peaks were being overlapped. Most of the peaks of PU, CA and zein have been overlapped in the PU–CA–zein-drug loaded nanofibers due to the relative similarity and shifting. When compared with pristine PU the peak intensities were observed to be decreased with CA and zein content. This may be due to the formation of hydrogen bonds among the components and the inter-hydrogen bonds formed between two different macromolecules were stronger than those formed between the molecules of the same polymer (Gonzalez, Guerrero, & Ortlz, 2000). Therefore, the inter-hydrogen bonds between PU, CA and zein were prone to formation. So the blending of CA, zein and drug with PU has been confirmed with FTIR.

The thermal stability of electrospun composite mats was evaluated by TGA. Fig. 3 shows the TGA curves of control PU, CA, PU–CA and blended PU–CA–zein-drug nanofiber mats. For the control PU sample, the initial decomposition temperature is 286 °C, which is higher than that of control CA mat at 275 °C. From the curves, it can be noted that the blended mat displayed single-stage degradation, which shows the better thermal stability of composite nanofibers. The decomposition temperature of PU–CA–zein-drug composite mat was lowered when compared to PU–CA, may be due to the lower thermal stability of zein in the composite mat. The amount of drug and zein in PU–CA nanofibers caused a reduction in the crystallinity of the polymer. During thermal decomposition, outer PU component can shield the inner CA, which may improve the thermal stability of blended mats. The data obtained in this study demonstrated a significant knowledge about the thermal stabilities between the PU–CA and PU–CA–zein-drug nanofibers in comparison to electrospun PU nanofibers.

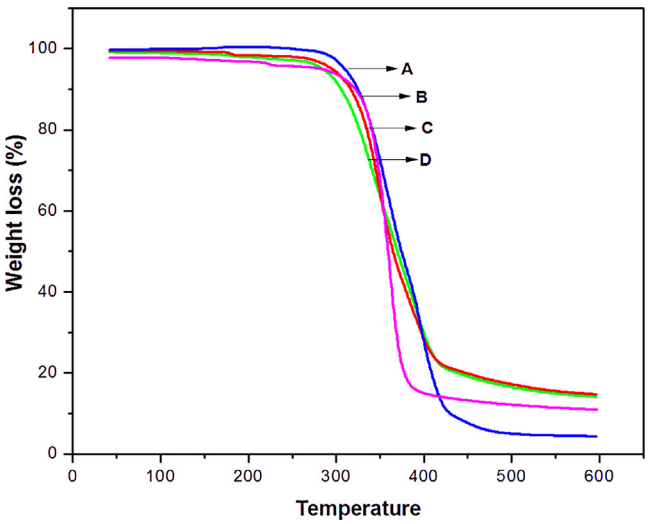

Fig. 3. TGA graphs of electrospun TGA graphs of electrospun (A) PU nanofiber mat, (B) CA nanofiber mat, (C) PU–CA nanofiber mat and (D) PU–CA–zein-drug nanofiber mat.

Fig. 4 shows the stress strain curves of pristine PU and composite electrospun mats. The mechanical properties for wound dressing materials are considered to be important because these materials need certain tensile strength, flexibility and elastic properties for handling and replacement. Pure PU presented excellent elasticity and the strength when compared to PU–CA–zein-drug composite nanofibers. In the case of PU–CA–zein-drug composite nanofibers the hardness increased as Young's modulus increased when compared to pristine PU nanofibers. A reasonable balance between flexibility and hardness can be achieved by blending different ratios of CA and zein. When compared with conventional wound dressing material, the soft and flexible nanofiber membranes were easier to handle and were detached easily from the wound sites for replacement. So our composite nanofiber material possesses enough properties to be used as a wound dressing material.

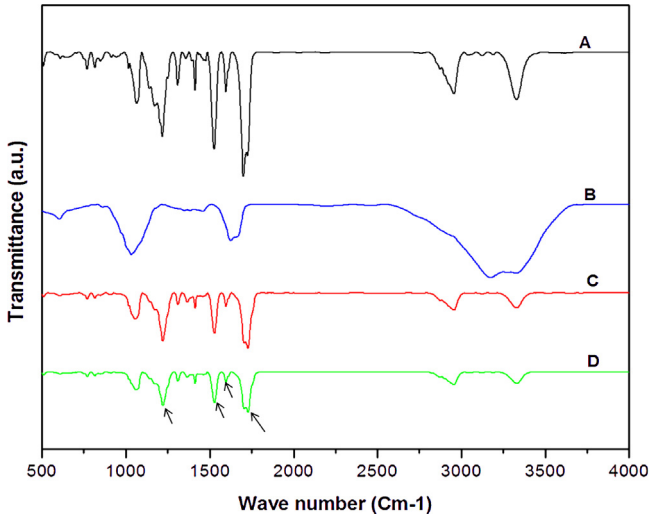

Fig. 2. FTIR spectra of electrospun (A) PU nanofiber mat, (B) streptomycin sulfate, (C) PU–CA–zein mat, and (D) PU–CA–zein-drug composite mat.

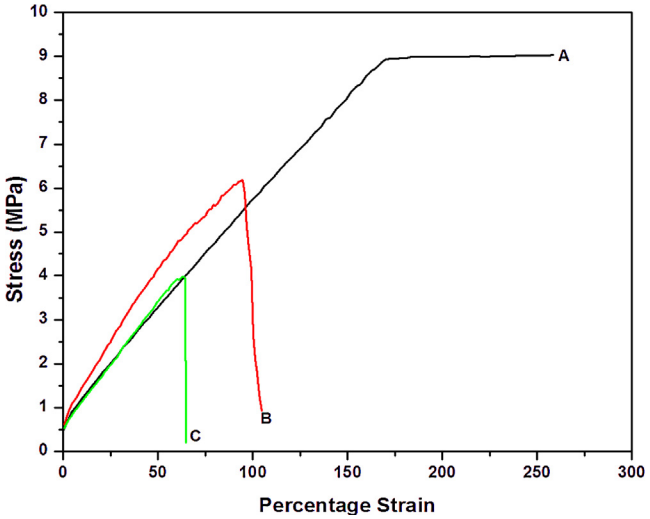

Fig. 4. Representative stress-strain curves of (A) PU nanofiber mat, (B) PU–CA–zein-drug nanofiber mat and (C) CA nanofiber mat.

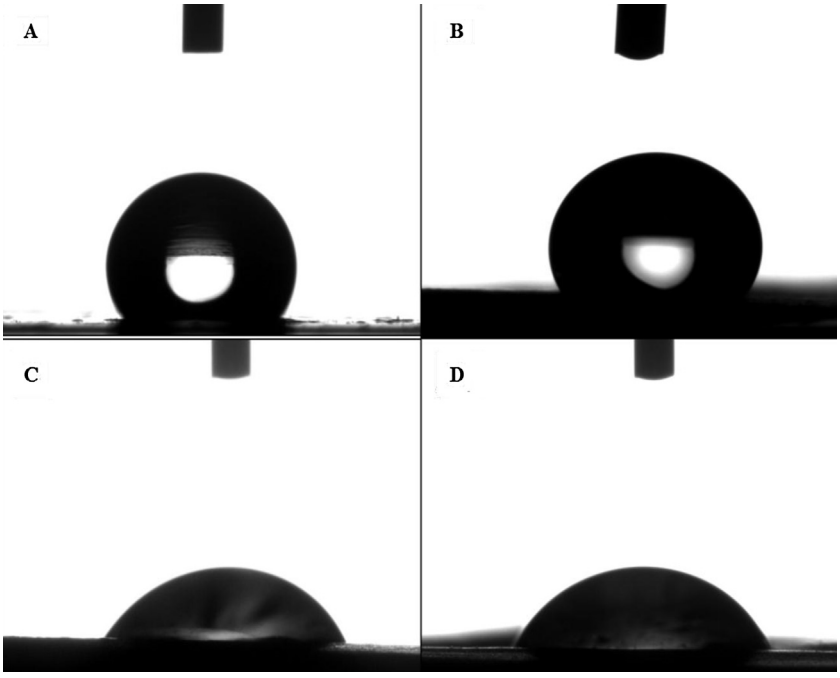

Fig. 5. Water contact angles of electrospun nanofibers from (A) PU nanofibrous mat, (B) PU–CA nanofibrous mat, (C) PU–CA–zein nanofibrous mat and (D) PU–CA–zein-drug composite nanofibrous mat.

The contact angle measurement details of composite nanofibers were shown in Fig. 5. As shown in Fig. 5(A), pristine PU nanofiber showed a hydrophobic nature with contact angle around $126.1 \pm 4^{\circ}$. Due to the addition of CA, the contact angle has been modified a little to $115.2 \pm 2^{\circ}$, attributed to the changed manner of the composite nanofiber toward hydrophilic in nature. The addition of CA to the PU caused this decrease in contact angle as shown in Fig. 5(B). But with the addition of zein to PU–CA composite nanofibers, drastically decreased the contact angle to $58.3 \pm 1^{\circ}$. This result demonstrates that addition of zein to PU–CA composite would result in a decrease of surface wettability for the electrospun nanofibers. The contact angle of the PU–CA–zein-drug composite nanofibers has been modified to $59.9 \pm 2^{\circ}$, may be due to the hydrophobic nature of the drug particles as given in Fig. 5(D). A more hydrophilic nanofiber surface will be helpful for the cell attachment but may result in poor fiber stability. Therefore, an optimized amount of zein should be taken in order to keep good surface wettability and fiber stability.

3.2. Evaluation of whole-blood clotting and platelet activation

In order to assess the hemostatic potential of nanofiber scaffolds, whole-blood clotting study was conducted. Fig. 6(A–C) shows the representative photographs of the blood clotting caused by the electrospun mats. The image of the composite mat before the addition of blood was given in Fig. 6(A). After the addition of blood, the nanofiber mat was fully covered with the blood as shown in Fig. 6(B). The composite mat showed a perfect blood clotting ability after 15 min incubation as depicted in Fig. 6(C). The optical density measurements showed that PU–CA–zein-drug composite nanoscaffold showed enhanced blood clotting ability in comparison with pristine PU as given in Fig. 6(D). This may be due to the interaction between cationic zein and negatively charged blood cells (Tseng, Tsou, Wang, & Hsu, 2013). This was further confirmed by the platelet activation analysis by SEM. Pristine PU did not activate the platelets while PU–CA–zein-drug composite nanoscaffold promoted platelet activation. The SEM images show that the activated platelets have spread all over the PU–CA–zein-drug composite nanofibrous mat surface as shown in Fig. 6(E and F). The uniform distribution of platelets along the composite mats indicate the perfect platelet adhesion and hence the enhanced clotting ability.

3.3. Antimicrobial test of the composite nanofibers

The bactericidal activity indicated a clear zone of inhibition within and around the drug loaded nanofiber mat after an overnight incubation of the agar plate at 37 °C. The growth inhibition rings of both gram-positive and gram-negative bacteria were measured. As shown in Fig. 7(A) for gram-positive bacteria *S. aureus* and *B. subtilis* the mean diameter of inhibition ring of drug loaded PU–CA–zein-drug composite nanofibers was around 8 mm and 15 mm, respectively. In case of gram-negative *E. coli*, *S. typhimurium* and *V. vulnificus* the diameters of the inhibition zones reached 12 mm, 10 mm and 10 mm, respectively, as shown in Fig. 7(B(1, 2, 3)). No bactericidal activity was detected for pristine PU and PU–CA–zein nanofibrous mats (Table 1). Fig. 7(C) shows the SEM image of bacterial attachment on pristine PU nanofibers. *S. aureus*

Table 1
Antibacterial data showing the diameter of zone of inhibition.

Bacterial strain	Pristine PU (zone of inhibition)	PU–CA–zein nanofibers (zone of inhibition)	PU–CA–zein-drug nanofibers (zone of inhibition)
E. coli	Nil	Nil	12 mm
Bacillus subtilis	Nil	Nil	15 mm
Vibrio vulnificus	Nil	Nil	10 mm
Salmonella typhimurium	Nil	Nil	10 mm
Staphylococcus aureus	Nil	Nil	8 mm

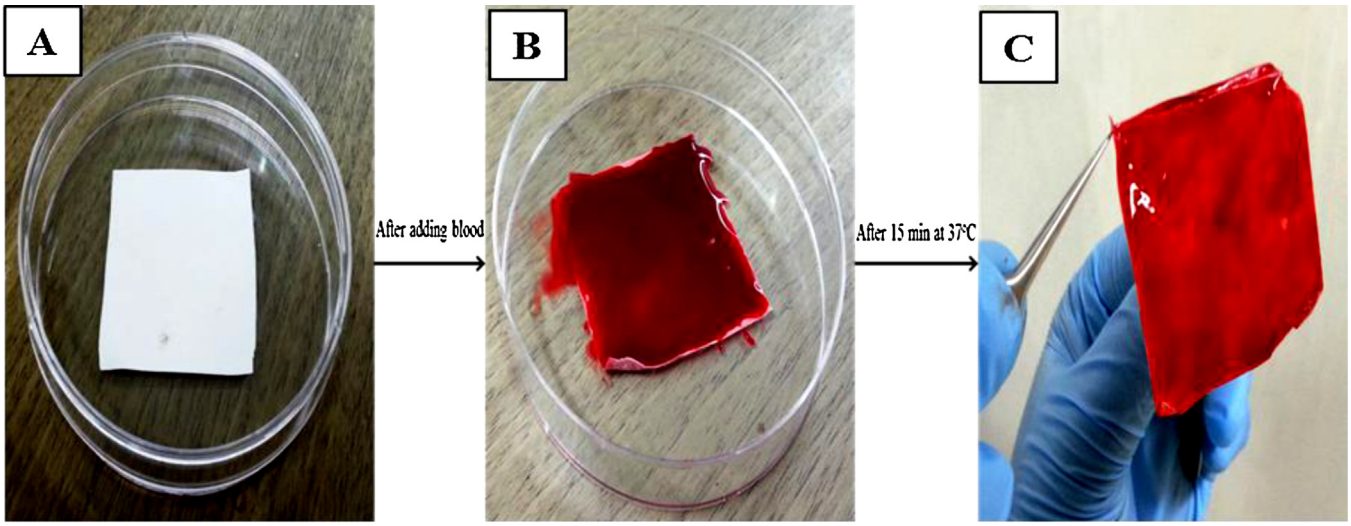
A
B
C
After adding blood
After 15 min at 37°C

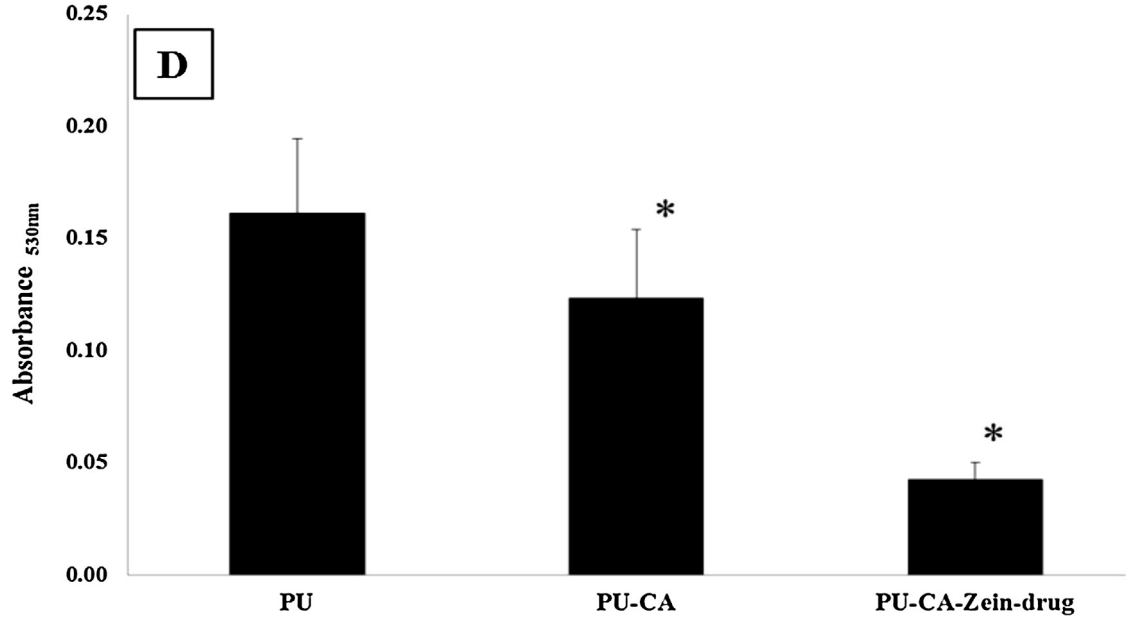
D
Absorbance 530nm
0.25
0.20
0.15
0.10
0.05
0.00
*
*
PU
PU-CA
PU-CA-Zein-drug

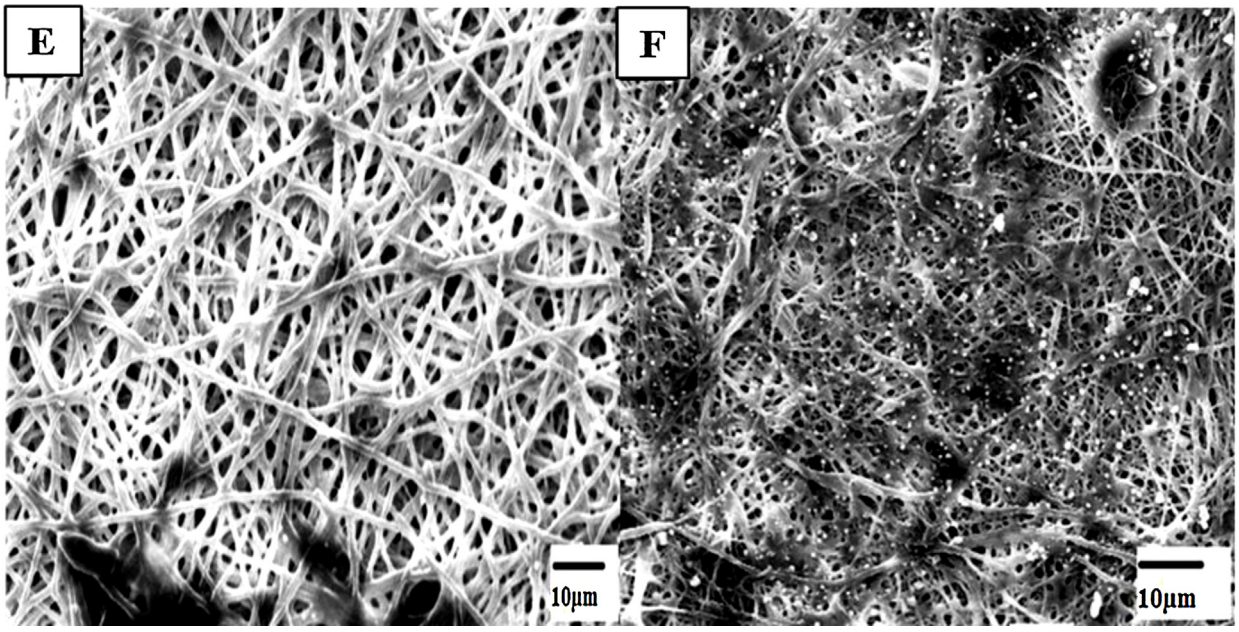
E
F
10μm
10μm

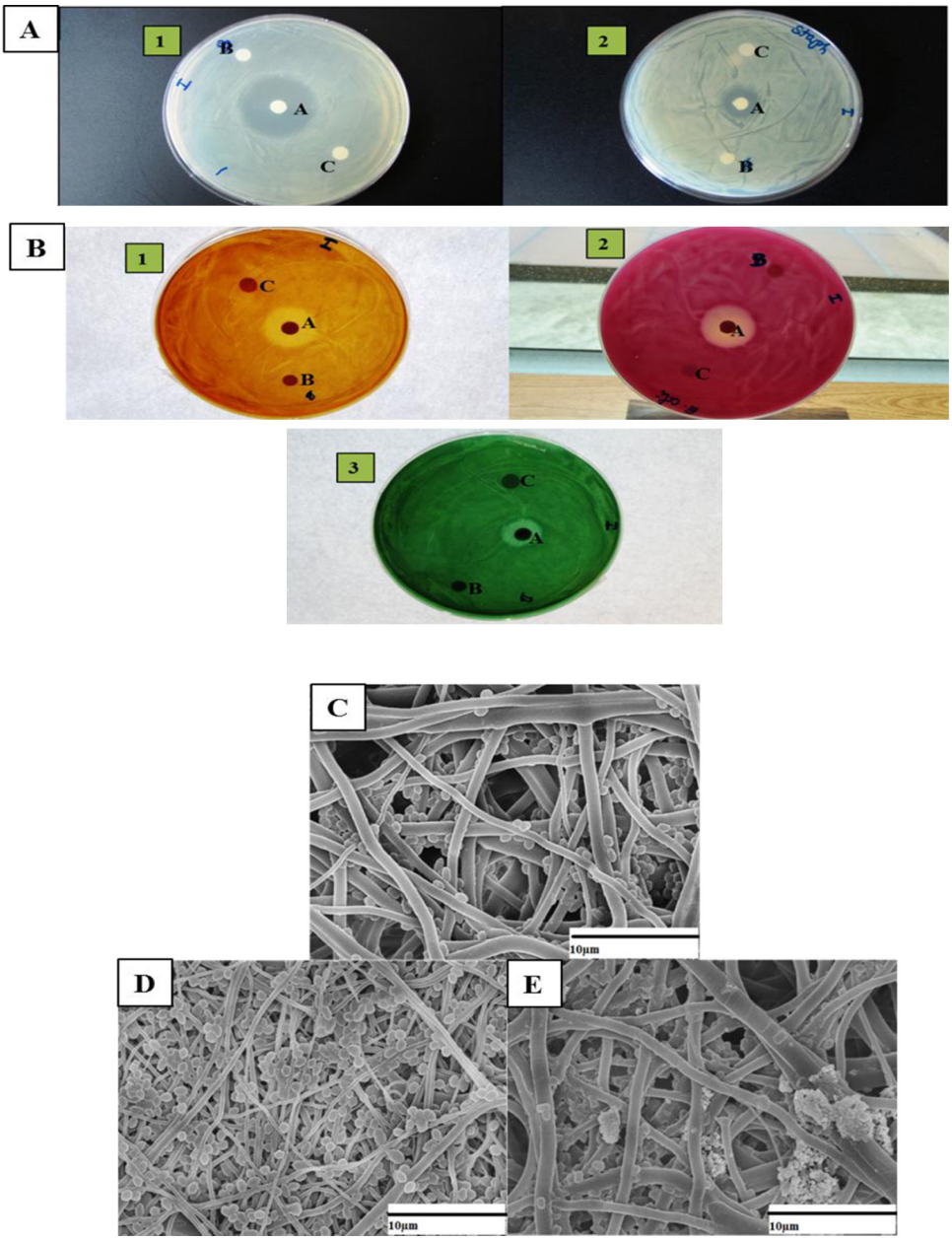

Fig. 7. (A) Bactericidal activity of PU–CA-zein–drug nanofibrous mat with (1) gram-positive *Bacillus subtilis*, (2) *Staphylococcus aureus*, (B) bactericidal activity of PU–CA-zein–drug nanofibrous mat with (1) gram-negative *Salmonella typhimurium*, (2) *Escherichia coli* and (3) *Vibrio vulnificus*, respectively. PU–CA-zein–drug, PU–CA and pristine PU discs were denoted as A, B and C, respectively, in the Petri plates. SEM images of bacterial attachment on nanofibers (C) *Staphylococcus aureus* attachment on PU nanofibrous mat, (D) *Staphylococcus aureus* and (E) *E. coli* attachment on PU–CA–zein-drug composite nanofibrous mat, respectively.

and *E. coli* showed more attachment toward PU–CA–zein-drug composite nanofibers compared to pristine PU nanofibers, owing to the improved antibacterial activity as shown in Fig. 7(D) and (E). Bacteria attached on the nanofibers with drug showed a distorted morphology while bacteria attached to the nanofibers without drug looked healthy thus showing that the nanomaterial is having good antimicrobial activity. Thus the drug loaded PU–CA–zein composite nanofibers showed excellent bactericidal activity against wide range of bacteria, therefore avoiding exogenous infections effectively. The decontamination of exogenous organisms is a critical factor for a wound healing material; the antibacterial property plays a crucial role for the electrospun-based wound dressing membranes. Wound infection caused by bacteria and other microorganisms often interrupts the healing process and leads to life threatening complications (Fuyin et al., 2013). The results showed that our composite mat is a good antibacterial membrane and it can be applied as a perfect wound dressing material.

Fig. 6. Photographs of the (A) PU–CA–zein nanofibrous mat, (B) blood on the PU–CA–zein composite mat, (C) clotted blood on the composite mat, (D) whole-blood clotting evaluation of nanofibrous mats (star symbols (*) represent the $p < 0.05$ level, indicating that the means are significantly different, compared to the control), SEM images of platelet activation of (E) PU nanofibrous mat and (F) PU–CA–zein-drug composite nanofibrous mat (white dots indicate the platelet adhesion on composite mat) respectively.

3.4. Cell study

The morphological appearances of cells on composite nanofiber mats were obtained after 3 and 6 days of culture for confirming the cell viability. Cell attachment studies via SEM images (Fig. 8) revealed that the cells were attached onto the drug loaded PU–CA–zein-drug composite nanofibrous scaffolds as well as to the pristine PU–CA–zein scaffolds and began to spread on the nanofibers. This result indicated the cytocompatible nature of the PU–CA–zein-drug composite nanofibrous scaffolds. Fig. 8 shows the SEM images of cell attachment manner on PU, PU–CA and PU–CA–zein-drug blended nanofibers. The SEM micrographs of fibroblasts on composite nanofiber scaffolds obtained on 3 and 6 days of culture showed a normal morphology of cell growth. Cell growth was higher on PU–CA and drug loaded PU–CA–zein-drug composite nanofibrous scaffolds than on PU nanofibers. PU, being a biocompatible, nontoxic, synthetic polymer, on blending with CA and zein provides a scaffold with improved bioactivity and cell affinity for skin tissue regeneration. It was observed that the cells were well incorporated into composite nanofibers compared to the pristine PU nanofibers. The hydrophilic nature of the PU–CA–zein scaffolds is another reason for better adhesion and proliferation of fibroblasts. From these data, one can clearly confirm the cell attachment and cell spreading in the nanofiber matrix. The porous nature of the composite nanofibrous scaffolds not only helped the cells to penetrate into the interior but also enhanced the transfer of oxygen and nutrients to cells. The cells that filtered into the interior of the drug loaded PU–CA–zein-drug composite nanofibrous scaffolds

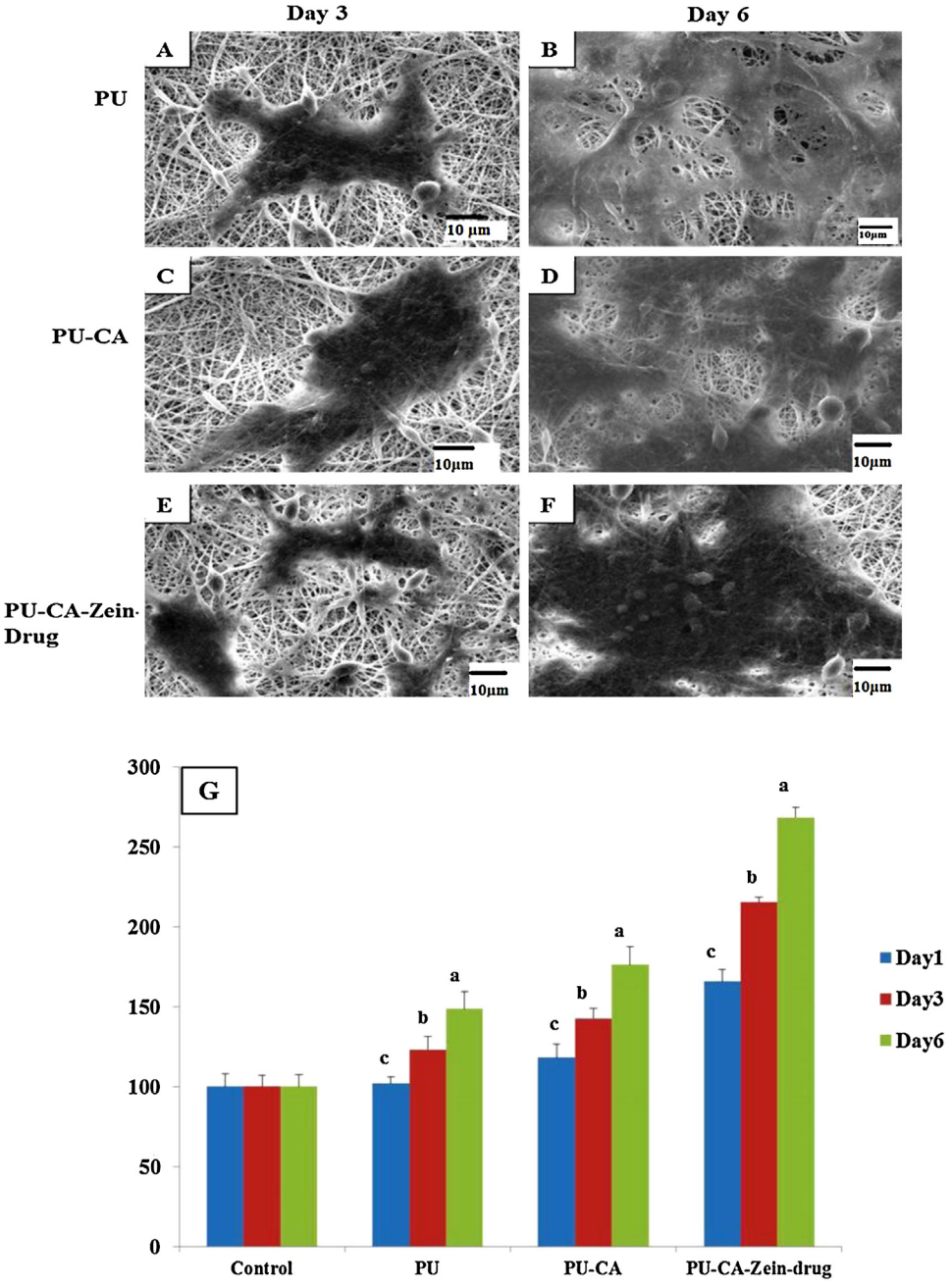

Fig. 8. SEM images showing the cell attachment on PU, PU–CA and PU–CA–zein-drug mats after day 3 (A, C, and E) and day 6 (B, D, and F), respectively, (G) MTT cell growth measurement assay. The viability of control cells was set at 100%. Values are mean ± SD. Values with different letters (a, b, c) are significantly different by ANOVA with Duncan's multiple range test at $p < 0.05$.

would be helpful for the vascularization, which is very essential in wound healing (Sowmya et al., 2012).

The proliferation of fibroblasts on neat PU and PU–CA and PU–CA–zein-drug matrices was evaluated by MTT assay on days 1, 3 and 6 (Fig. 8(G)). PU–CA–zein-drug composite nanofibrous scaffolds were more suitable for the growth of fibroblasts as compared to PU–CA and PU scaffolds, attaining a significant level of increase in cell proliferation after 3 and 6 days of culture. The presence of zein enhanced the bioactivity and cell affinity of the composite scaffolds as seen in Fig. 8(G). More cells were able to attach and grow on the zein loaded nanofibers as the composite nanofibers become more hydrophilic and bioactive. Results clearly indicate that the presence of zein highly accelerates the proliferation of fibroblasts on composite scaffolds. A large number of interconnected pores and the rough surface of the nanofibrous membrane and enhanced cytocompatibility of zein support the proliferation and quicker regeneration of cells, which is very essential in wound healing.

4. Conclusion

In summary, we successfully obtained drug loaded PU–CA–zein blended composite nanofibers by using the electrospinning process. Blending of CA and zein with PU resulted in improved physiological and biological characteristics. Thus obtained composite mat was characterized with various methods. PU–CA–zein-drug composite nanofibrous scaffolds showed enhanced blood clotting and excellent platelet activation ability. In vitro cytocompatibility studies revealed that the scaffolds showed enhanced cell viability and infiltration. In vitro antibacterial activity studies proved that the antibacterial potential of the prepared composite scaffold. All these studies indicated that these advanced PU–CA–zein-drug composite nanofibrous scaffolds can be used for burn, chronic and diabetic wound infections.

Acknowledgement

This research was supported by grants from the Basic Science Research Program through the National Research Foundation of Korea (NRF) funded by the Ministry of Education, Science and Technology (Project nos. 2013-012911 and 2013R1A2A2A04015484).

References

Afeesh, R., Tirupathi, P. B., Gnanasekaran, G., Nirmala, R., Barakat, N. A. M., Cha, Y. S., et al. (2012). Wound-dressing materials with antibacterial activity from electrospun polyurethane-dextran fiber mats containing Ciprofloxacin HCl. *Carbohydrate Polymers*, *90*, 1786–1793.

Bauer, R. W., Kirby, M. D. K., Sherris, J. C., & Turck, M. (1996). Antibiotic susceptibility testing by standard single disc diffusion method. *American Journal of Clinical Pathology*, *45*, 493–496.

Fang, J., Niu, H., Lin, T., & Wang, X. G. (2008). Applications of electrospun nanofibers. *Chinese Science Bulletin*, *53*, 2265–2286.

Forato, L. A., Doriguetto, A. C., Fischer, H., Mascarenhas, Y. P., Craievich, A. F., & Colnago, L. A. (2004). Conformation of the Z19 prolamin by FTIR, NMR, and SAXS. *Journal of Agricultural and Food Chemistry*, *52*, 2382–2385.

Fuyin, Z., Shige, W., Shihui, W., Mingwu, S., Meifang, Z., & Xiangyang, S. (2013). Characterization and antibacterial activity of amoxicillin-loaded electrospun nano-hydroxyapatite/poly (lactic-co-glycolic acid) composite nanofibers. *Biomaterials*, *34*, 1402–1412.

Glasser, W. G. (2004). Prospects for future applications of cellulose acetate. *Macromolecular Symposia*, *208*, 371–394.

Gong, S., Wang, H., Sun, Q., Xue, S. T., & Wang, J. Y. (2006). Mechanical properties and in vitro biocompatibility of porous zein scaffolds. *Biomaterials*, *273*, 793–799.

Gonzalez, V., Guerrero, C., & Ortlz, U. (2000). Chemical structure and compatibility of polyamide–chitin and chitosan blends. *Journal of Applied Polymer Science*, *78*, 850–857.

Jayakumar, R., Menon, D., Manzoor, K., Nair, S. V., & Tamura, H. (2010). Biomedical applications of chitin and chitosan nanomaterials – A short review. *Carbohydrate Polymers*, *82*, 227–232.

Jayakumar, R., Prabaharan, M., Sudheesh, K. P. T., Nair, S. V., & Tamura, H. (2011). Biomaterials based on chitin and chitosan in wound dressing applications. *Biotechnology Advances*, *29*, 322–337.

Jiang, Z., Yuan, K. J., Li, S. F., & Chow, W. K. (2006). Study of FTIR spectra and thermal analysis of polyurethane. *Spectroscopy and Spectral Analysis*, *26*, 624–628.

Jiang, Q., Reddy, N., & Yang, Y. (2010). Cytocompatible crosslinking of electrospun zein fibers for the development of water stable tissue engineering scaffolds. *Acta Biomaterialia*, *6*, 4042–4051.

Kanjanapongkul, K., Wongsasulak, S., & Yoovidhya, T. J. (2010). Investigation and prevention of clogging during electrospinning of zein solution. *Journal of Applied Polymer Science*, *118*, 1821–1829.

Kong, B., & Xiong, Y. L. (2006). Antioxidant activity of zein hydrolysates in a liposome system and the possible mode of action. *Journal of Agricultural and Food Chemistry*, *54*, 6059–6068.

Lakshmi, R. L., Shalumon, K. T., Sreeja, V., Jayakumar, R., & Nair, S. V. (2010). Preparation of silver nanoparticles incorporated electrospun polyurethane nano-fibrous mat for wound dressing. *Journal of Macromolecular Science Pure and Applied Chemistry*, *47*, 1012–1018.

Liu, X., Sun, Q., Wang, H., Zhang, L., & Wang, J. Y. (2005). Microspheres of corn protein, zein, for an ivermectin drug delivery system. *Biomaterials*, *26*, 109–115.

Madhumathi, K., Sudheesh, K. P., Abilash, S., Sreeja, V., Tamura, H., & Manzoor, K. J. (2010). Development of novel chitin/nanosilver composite scaffolds for wound dressing applications. *Journal of Materials Science: Materials in Medicine*, *21*, 807–813.

Ong, S. Y., Wu, J., Moochhala, S. M., Tan, M. H., & Lu, J. (2008). Development of a chitosan-based wound dressing with improved hemostatic and antimicrobial properties. *Biomaterials*, *29*, 4323–4332.

Richard, J. L., & Shama, G. (2005). Direct FTIR assay of streptomycin in agar. *Biotechnology Letters*, *27*, 1629–1631.

Shukla, R., & Cheryan, M. (2001). Zein: The industrial protein from corn. *Industrial Crops and Products*, *13*, 171–192.

Sowmya, S., Jayakumar, R., Chennazhi, K. P., Levorson, E. J., Mikos, A. G., & Nair, S. V. (2012). Multiscale fibrous scaffolds in regenerative medicine. *Advances in Polymer Science*, *246*, 1–10.

Sudheesh, K. P. T., Lakshmanan, V. K., Anilkumar, T. V., Ramya, C., Reshmi, P., Unnikrishnan, A. G., et al. (2012). Flexible and microporous chitosan hydrogel/nano ZnO composite bandages for wound dressing: In vitro and in vivo evaluation. *Applied Materials and Interfaces*, *4*, 2618–2629.

Tseng, H. J., Tsou, T. L., Wang, H. J., & Hsu, S. H. (2013). Characterization of chitosan-gelatin scaffolds for dermal tissue engineering. *Journal of Tissue Engineering and Regenerative Medicine*, *7*, 20–31.

Yu, D. G., Li, X. Y., Xia, W., Wei, C., Liao, Y. Z., & Li, Y. (2013). Zero-order drug release cellulose acetate nanofibers prepared using coaxial electrospinning. *Cellulose*, *20*, 379–389.